KIR2DS2 recognizes conserved peptides derived from viral helicases in the context of HLA-C

Mohammed M Naiyer[1], Sorcha A Cassidy[1,2], Andrea Magri[3, 4], Vanessa Cowton[3], Kevin Chen[1], Salah Mansour[1], Hariklia Kranidioti[1], Berenice Mbirbindi[1], Pauline Rettman[1], Scott Harris[5], Liam J Fanning[6], Arend Mulder[7], Franz H J Claas[7], Andrew D Davidson[8], Arvind H Patel[3], Marco A Purbhoo[2], Salim I Khakoo[1*].

[1] Clinical and Experimental Sciences, Faculty of Medicine, University of Southampton, Southampton General Hospital, Tremona Road, Southampton S016 6YD, UK

[2]Section of Hepatology, Division of Medicine, Imperial College London, South Wharf Road, London, W2 1PG, UK

[3]MRC – University of Glasgow Centre for Virus Research, Garscube Campus, 464 Bearsden Road, Glasgow G61 1QH, UK

[4]Department of Translational Medicine, Università del Piemonte Orientale, Novara, Italy.

[5]Department of Statistics, Population and Primary Care Medicine, Faculty of Medicine, University of Southampton, Southampton General Hospital, Tremona Road, Southampton S016 6YD, UK

[6]Department of Medicine, University College Cork, Cork, Ireland.

[7]Department Immunohaematology and Blood transfusion, Leiden University Medical Center, PO Box 9600, 2300RC LEIDEN, The Netherlands

[8]School of Cellular and Molecular Medicine, Biomedical Sciences Building, University of Bristol, Bristol, BS8 1TD, UK

Address Correspondence to:

*Salim I Khakoo
Faculty of Medicine
University of Southampton
Mailpoint 811
Level E South Academic Block
Southampton General Hospital
Tremona Road
Southampton
SO16 6YD
Tel 023 8079 6671/5099
Fax: 023 8051 1761
E-mail: S.I.Khakoo@soton.ac.uk

One sentence summary:

KIR2DS2, an activating natural killer cell receptor recognizes highly conserved peptides derived from the RNA helicases of pathogenic flaviviruses.

Abstract

Killer cell immunoglobulin-like receptors (KIR) are rapidly evolving species-specific natural killer cell receptors associated with protection against multiple different human viral infections. We report that the activating receptor KIR2DS2 directly recognizes viral peptides derived from conserved regions of flaviviral superfamily 2 RNA helicases in the context of MHC class I. The peptide LNPSVAATL, from the HCV helicase, binds HLA-C*0102 leading to NK cell activation through engagement of KIR2DS2. Similarly, HLA-C*0102 presents highly conserved peptides from the helicase motif 1b region of related flaviviruses, including dengue, Zika, yellow fever and Japanese encephalitis viruses, to KIR2DS2. These flaviviral peptides all contain an "MCHAT" motif, which is present in 61 out of 63 flaviviruses. LNPSVAATL is also highly conserved across HCV genotypes and mutation of this epitope is poorly tolerated by HCV. KIR2DS2 recognizes endogenously presented helicase peptides and KIR2DS2 is sufficient to inhibit HCV and dengue virus replication in the context of HLA-C*0102. Targeting short, but highly conserved, viral peptides provide non-rearranging innate immune receptors with an efficient mechanism to recognize multiple, highly variable pathogenic RNA viruses.

Introduction

Natural killer (NK) cells are critical determinants in the innate immune response to a number of globally-important viral infections including HIV, hepatitis C virus, dengue and Chikungunya virus (*1-4*). Their functions are controlled by non-rearranging immune receptors many of which are well conserved, consistent with a role in innate immunity. The killer cell immunoglobulin-like receptors (KIR) are a rapidly evolving family of NK cell receptors that exhibit substantial population diversity. They have peptide:MHC class I specificity, and certain combinations of KIR and their MHC class I ligands have been associated with the outcome of a number of viral infections including, the inhibitory receptor KIR2DL3 and hepatitis C, and the activating receptor KIR3DS1 and HIV (*4, 5*).

The KIR have evolved rapidly since the divergence of humans from chimpanzees, in a manner indicative of pathogen-mediated selection. One mechanism by which the KIR contribute to recognition of pathogens has been identified for inhibitory KIR as related to downregulation of MHC class I (*6*). Conversely, there is little understanding of how activating KIR can recognize pathogens. Recent work has shown that KIR3DS1, which shares sequence homology with HLA-B specific inhibitory KIR3DL1, binds open conformers of HLA-F and this may result in inhibition of HIV infection (*7*). However, the mechanisms by which the activating KIR with putative HLA-C ligands recognize pathogens remain enigmatic (*8*).

Human KIRs bind subsets of HLA class I ligands and engage both the HLA class I heavy chain and the bound peptide. Furthermore, changes in the peptide content of HLA class I can abrogate KIR-mediated inhibition of NK cells, demonstrating a mechanism for KIR-associated NK cell activation distinct from HLA class I down-regulation (*9*). KIR2DL2 and KIR2DL3 are inhibitory KIRs with a predominant specificity for the group 1 HLA-C allotypes

(HLA-C1). Both these inhibitory receptors have similar specificities for peptide:MHC, as could be predicted from the high sequence homology of their extra-cellular domains (*10*). The activating receptor KIR2DS2 also has ~98% amino acid identity in the ligand binding domains to KIR2DL2 and KIR2DL3, and is in strong linkage disequilibrium with KIR2DL2. Despite this shared sequence homology, it has been difficult to identify binding of KIR2DS2 to HLA-C. One of the key differences between KIR2DS2 and KIR2DL2/KIR2DL3 is the presence of a tyrosine, as compared to a phenylalanine, residue at position 45 and this is thought to significantly affect binding of KIR2DS2 to HLA-C (*11*). Low level binding of KIR2DS2 to HLA-C in combination with an Epstein-Barr virus (EBV) peptide was detected by surface plasmon resonance (*12*). More recently, KIR2DS2 has been demonstrated to have peptide specific binding to HLA-A*1101, an HLA class I allele which binds a number of diverse KIR including KIR2DS4 and KIR3DL2 (*13, 14*). KIR2DS2 has also been shown to bind cancer cell lines in a ß2-microglobulin independent manner (*15*). Nonetheless, based on the high sequence homology of KIR2DS2 with KIR2DL2 and KIR2DL3, we sought to determine if KIR2DS2 was also an HLA-C restricted peptide specific receptor.

Results

KIR2DS2 recognizes the HCV peptide LNPSVAATL in the context of HLA-C*0102

Immunogenetic analyses by Thio *et al.* have identified HLA-C*0102 to be protective in the context of chronic HCV infection (*16*). Based on this observation, we used HLA-C*0102 as a template allele to identify peptides from HCV to determine how they may modulate NK cell function. We screened the HCV genotype 1b genome (AF313916.1) for potential HLA-C*0102 binding peptides using the algorithms ADT, Net-MHC pan and KISS, coupled with a manual scan using the known HLA-C*0102 motif xxPxxxxxL (*17*). We identified eight peptides for further study (**Table S1**). We used the TAP-deficient 721.174 cell line, which expresses HLA-C*0102 naturally, to present the HCV peptides in binding and functional assays. These cells are deficient in the TAP protein and hence can be used to present exogenous peptide to lymphocytes (*18*). Analysis of binding to HLA-C*0102 using peptide titrations demonstrated that four peptides (LLPRRGPRL, AQPGYPWPL, LSPHYKVFL, RAYLNTPGL) had a low affinity for HLA-C*0102, not reaching saturation point at 100μM, one (VLPCSFTTL) had an affinity comparable to the endogenously presented peptide VAPWNSLSL, and the remainder (LSPRPVSYL, LNPSVAATL, ARPDYNPPL) had an intermediate affinity for HLA-C*0102 (**Fig. S1**).

In order to determine how these peptides modulate NK cell reactivity, we used the 721.174 cells. The CD158b epitope includes the KIR2DL2, KIR2DL3 and KIR2DS2 proteins and therefore marks NK cells with specificity for HLA-C*0102. We identified one peptide LLPRRGPRL that inhibited the activation of CD158b+ NK cells, but the remainder of the peptides had no effect on NK cell degranulation relative to the “no peptide” control (**Fig. S2**). In the absence of peptide there is activation of CD158b-positive NK cells by 721.174 such that 25-30% NK cells express CD107a (Fig. 1A and 1B). In order to identify specific activation of KIR2DS2-positive NK cells, we reduced the background activation of CD158b-

positive NK cells by using an inhibitory peptide VAPWNSFAL, and testing the ability of the peptides to activate NK cells relative to this strong inhibitory signal. We used VAPWNSFAL as it was the strongest inhibitory peptide that we identified in a peptide screening assay for KIR binding and NK cell inhibition (*9*). From an initial screening assay using three unselected donors, we identified two peptides, LNPSVAATL (LNP) and VLPCSFTTL (VLP), which activated CD158b+ NK cells relative to VAPWNSFAL alone (**Fig. 1A**).

As CD158b marks the inhibitory receptors KIR2DL2 and KIR2DL3, and the activating receptor KIR2DS2, we stratified the donors by KIR genotype: *KIR2DL2*$^{+}$*KIR2DS2*$^{+}$*KIR2DL3*$^{-}$ (*KIR2DL2/S2* homozygous) and *KIR2DL2*$^{-}$*KIR2DS2*$^{-}$*KIR2DL3*$^{+}$ (*KIR2DL3* homozygous). VLP activated CD158b-positive NK cells relative to VAPWNSFAL alone in both *KIR2DL2*$^{+}$*/S2*$^{+}$*/L3*$^{-}$ donors and *KIR2DL2*$^{-}$*/S2*$^{-}$*/L3*$^{+}$ donors (**Fig. 1B**). In contrast, the effect of LNP on CD158b-positive NK cells was present for *KIR2DL2*$^{+}$*/S2*$^{+}$*/L3*$^{-}$ donors, but not *KIR2DL2*$^{-}$*/S2*$^{-}$*/L3*$^{+}$ donors (**Figs. 1B and 1C**). Conversely no differences were found for the CD158b-negative NK cells for either groups of donors (**Fig. 1D**). This indicates that the increase in degranulation was related either to KIR2DL2 or to KIR2DS2. KIR2DL2^{+} NK cells are less responsive to changes in peptide content of MHC class I than KIR2DL3^{+} NK cells (*19*). Therefore, we reasoned that this change in degranulation was related to NK cell activation through engagement of KIR2DS2.

In order to map this specificity more closely, we cloned NK cells from a *KIR2DL2*$^{+}$*KIR2DS2*$^{+}$*KIR2DL3*$^{-}$ donor. We tested three KIR2DS2+ NK cell clones against the 721.174 cells (**Fig. S3**). We found that although LNP augmented lysis of 721.174 cells by KIR2DS2-positive NK cell clones, background levels of killing against targets in the absence of peptide were high. We therefore sought an alternative strategy using the KIR-negative cell line NKL. We transfected NKL cells with either KIR2DS2 or KIR2DL2 and used them as

effector cells. We also generated 721.221 target cells stably expressing either HLA-C*0102 alone or HLA-C*0102 and LNP together. In cytotoxicity assays NKL-2DS2 cells lysed 721.221:C*0102 cells to a similar level as untransfected NKL cells, but lysed LNP expressing 721.221:C*0102 cells significantly better than 721.221:C*0102 cells without LNP (**Fig. 1E and 1F**). Thus LNP specifically activates NKL cells expressing KIR2DS2, but has no effect of KIR2DL2-positive NK cells. As there were similar levels of killing of 721.221:C*0102 cells by NKL-2DS2 and NKL cells, this observed increased level of lysis is not related to a generalized increase in baseline cytolytic activity of the NKL-2DS2 cell line against 721.221 cells, but to specific recognition of the combination of LNPSVAATL and HLA-C*0102 by KIR2DS2.

LNPSVAATL engages KIR2DS2, but not KIR2DL2

In order to confirm the reactivity of KIR2DS2 with HLA-C*0102:LNP, we made a KIR2DS2 tetramer. In a binding assay we detected low-level, but consistent and significant binding of the KIR2DS2 tetramer to the peptide LNPSVAATL ($p<0.001$) as compared to the naturally eluted peptide VAPWNSLSL and also KIR2DS2 binding to the peptides VAPWNSATL and VAPWNAATL (**Fig. S4**). This is in line with previous observations that positions seven and eight of the HLA class I peptide are important for KIR binding, as has been observed for the inhibitory KIR. As the binding of the tetramer was at a low level (~1.5 times background), we used a clustering assay to determine if a cell-cell contact assay could detect specific recognition of LNP by KIR2DS2. Transfectants of the Ba/F3 cell line expressing either KIR2DL2 or KIR2DS2 were used to investigate receptor clustering (*20*). These are murine B cells and hence do not express other human NK cell activating receptors. The Ba/F3 transfectants were co-incubated with 721.174 cells pulsed with peptide. LNP induced clustering of KIR2DS2, but not KIR2DL2, whereas the inhibitory peptide VAPWNSFAL induced clustering only of KIR2DL2 (**Figs. 2A and B**).

To further determine if the interaction of LNP with KIR2DS2 led to NK cell activation, we studied signalling in the NKL cell lines. Activating KIRs transduce positive signals through the adapter molecule DAP12 and antibody cross-linking of KIR2DS2 has been shown to lead to DAP12 phosphorylation (*20*). We therefore tested whether LNP could lead to activation of NK cells via DAP12. Immunoprecipitation (IP) of KIR2DS2 from NKL-2DS2 cells co-cultured with 721.174 cells in the presence or absence of peptide, demonstrated LNP-induced enhanced tyrosine phosphorylation of the co-immunoprecipitated DAP12, consistent with NK cell activation (**Fig. 2C**). Moreover, the presence of LNP augmented tyrosine phosphorylation of the downstream guanine nucleotide exchange factor Vav1 in NKL-2DS2 cells, but had no effect on KIR2DL2 signalling in NKL-2DL2 cells (**Fig. 2D**). We further tested whether KIR2DL2 could bind LNP in the context of C*0102 using a KIR2DL2-Fc fusion construct. Consistent with the functional experiments, there was no direct binding of a KIR2DL2 fusion construct to LNP-pulsed 721.174 cells (**Fig. 2E**). Taken together these data demonstrate that LNP specifically activates KIR2DS2^{+} NK cells through the DAP12-Vav1 pathway, but has no effect on KIR2DL2^{+} NK cells, establishing it as a peptide that discriminates an activating KIR from its closely related inhibitory counterpart.

KIR2DS2 recognizes LNPSVAATL in the context of HCV infection

Having observed that KIR2DS2 recognized LNP in the context of HLA-C*0102 as both exogenously and endogenously loaded peptide, we wanted to test if it could also recognize LNP in the context of HCV replication. To do this we generated an HUH7 cell line stably expressing the HCV sub-genomic replicon N17 (JFH1ΔE1E2-luc) and also transfected in HLA-C*0102. N17 contains the full length HCV genome without the envelope proteins, and replicates as a wild-type virus, and hence it is considered that it produces proteins to a similar level as wild-type virus (*21*). It also has a luciferase gene incorporated within the HCV

construct to allow assessment of replication by a luciferase assay. HUH7 is a hepatoma cell line that expresses HLA-A*1101, but not HLA-B or HLA-C and is permissive for HCV replication (*22*). We used the transfected NKL cell lines to assess the potential for KIR2DS2 to specifically inhibit replication of N17 in this system. NKL-2DS2 inhibited HCV replication at low E:T ratios (0.01:1) in the HLA-C*0102-expressing HUH7 cells to a significantly greater extent than parental NKL cells or NKL-2DL2 cells. (**Fig. 3A right panel**). Conversely in the parental HUH7 cell line, that is HLA-C negative, NKL, NKL-2DL2 and NKL-2DS2 inhibited HCV replication to similar levels (**Fig. 3A**) suggesting that KIR2DS2 requires the presence of HLA-C to inhibit HCV replication.

To investigate the role of the LNP peptide in the inhibition of HCV replication by KIR2DS2 we made non-conservative aspartate variants of the N17 replicon at the HLA-binding anchor residues P3 and P9, and the putative KIR binding residues, P7 and P8 (*17*). Mutation of P9 retained HCV replication to wild-type levels, but mutation of the P3, P7 or P8 residues in this epitope profoundly inhibited replication of the N17 replicon viral RNA to a level similar as that of the non-replicating control which has a lethal “GND” polymerase mutation (*23*) (**Fig. 3B**). We therefore performed inhibition of replication assays using only the P9 leucine to aspartate N17 variant (L9D). In these assays there was no specific effect of KIR2DS2 noted (**Fig. 3C**) suggesting that KIR2DS2 recognition of HCV in the context of HLA-C*0102 is dependent on the LNP epitope.

To test the HLA-C specificity of this response we transfected HUH7 cells, expressing either the N17 replicon or the mutated N17-L9D replicon, with HLA-C*0304. NKL-2DS2 inhibited HCV replication to a significantly greater extent than NKL-2DL2 or the parental NKL cell lines at all E:T ratios tested (**Fig. 3D**). However, this was not related to the LNP peptide as NKL-2DS2 also inhibited replication of the N17-L9D replicon to a similar extent. Importantly LNP

was unable to stabilize HLA-C*0304 in a peptide stabilization assay using 721.221:HLA-C*0304 cells transfected with ICP47 which blocks transporter associated with antigen processing (TAP) function (**Fig. 3E**). Furthermore, using the same cell lines to present peptide, LNP did not engage KIR2DS2 in the context of HLA-C*0304 in tetramer-binding or Vav1 phosphorylation assays (**Fig. 3F and 3G**). In order to generate a positive control peptide for this experiment, we tested P7 and P8 derivatives of the naturally processed HLA-C*0304-binding peptide, GAVDPLLAL, guided by our current work and also that of Liu *et al* (*13, 24*). GAVDPLLAL, GAVDPLAWL and GAVDPLATL all stabilised HLA-C*0304, but only GAVDPLAWL induced binding of the KIR2DS2 tetramer to HLA-C*0304 and Vav1 phosphorylation (**Fig. 3E-G**). Thus KIR2DS2 has a broad peptide:HLA-C specificity and it is likely that there are other HCV peptides that can be presented by HLA-C*0304 and recognized by KIR2DS2.

LNPSVAATL is a highly conserved peptide

HCV is an RNA virus with high sequence variability due to a lack of a proof-reading capability of its RNA polymerase. We therefore assessed whether there was a clinical correlate to the defective replication of replicons with LNP variants. We observed that the LNP epitope is highly conserved across HCV genotypes which in general differ by up to 30% in sequence identity (**Table S2**). Indeed, genotype 5 HCV, the only genotype with a consistent variation of this epitope, has a leucine to phenylalanine variant at P9 consistent with our finding in the replication assays that variation at P9 of the LNP epitope does not affect HCV replication. Furthermore the LNP epitope is conserved across 878 (98.5%) of the 891 HCV NS3 sequences deposited in the Los Alamos HCV database (http://hcv.lanl.gov). Thus, a lack of natural variation in this region implies that, *in vivo*, mutation of LNP is relatively poorly tolerated and marks it as a viable target for a non-rearranging immune receptor.

Furthermore, structural analysis demonstrates LNP is located within the RNA helicase domain of the HCV NS3 protein in the Ia motif and that the LNP peptide is in the RNA binding region of this motif, consistent with its relative lack of variation (*25*). Thus, it is in a critical functional region of HCV.

To investigate if KIR2DS2 was associated with the outcome of HCV infection on a genetic basis, we performed logistic regression analysis of: putative activating KIR:HLA combinations (*KIR2DS1:HLA-C2*, *KIR2DS2:HLA-A*11*, *KIR2DS2:HLA-C1*, *KIR3DS1:HLA-B*^{Bw4}) and control activating KIR:HLA combinations (*KIR2DS1:HLA-C1*, *KIR2DS2:HLA-C2*), together with key protective (*KIR2DL3:HLA-C1* homozygosity) and susceptibility (*KIR2DS3*) factors in our UK Caucasian population with resolved (n=120) or chronic (n=216) HCV infection (*4*). *KIR2DS2* in combination with *HLA-C1* was protective against chronic HCV infection (p=0.033, OR=2.06 95% CI=1.06-4.02), but no association was found between *KIR2DS2* in combination with *HLA-A*11* and the outcome of HCV infection (**Table 1**). We also noted that *KIR3DS1* in combination with *HLA-B*^{Bw4} was protective, but none of the control combinations were associated with the outcome of HCV infection. Thus, in HCV infection, group 1 *HLA-C* alleles are protective in combination with both KIR A (*KIR2DL3*) and KIR B (*KIR2DS2*) centromeric haplotypes.

A highly conserved peptide from multiple flaviviruses contains the "AT" KIR2DS2-binding motif

HCV is a member of the *Flaviviridae* family, which incorporates viruses within the genus *Flavivirus* that include globally important pathogens such as Zika, dengue, yellow fever, Japanese encephalitis and West Nile viruses. Similar to HCV, these viruses all encode an RNA helicase belonging to superfamily 2 (SF2) as a C-terminal domain of the NS3 protein (*26*). However, as the LNP peptide is not conserved amongst these viruses we sought

additional HLA-C*0102-binding peptides that may engage KIR2DS2. We screened the viral genomes from these viruses using NET MHCpan 2.8 and a percentage rank cut-off for binding of 2. We identified putative HLA-C*0102 -binding peptides from the helicases of these viruses that had both the HLA-C*0102 binding motif and the "AT" KIR2DS2-binding motif (**Table S3**). These peptides all contained a highly conserved MCHAT sequence from the NS3 Ib motif that is completely conserved amongst 61 out of 63 viruses within the genus *Flavivirus* regardless of the species tropism of the virus (**Fig. 4** and **Table S4**). Interestingly, using a blast search (https://blast.ncbi.nlm.nih.gov/Blast.cgi), this sequence is not found intact within the human genome.

KIR2DS2 recognizes conserved peptides from Flavivirus helicases

We then assessed KIR2DS2 binding to peptides containing this conserved "MCHAT" peptide motif. We identified representative peptides from key human pathogens including Zika virus (ZIKV) and dengue viruses (DENV) (IVDLMCHATF: both ZIKV $NS3_{255\text{-}264}$ [BAP47441.1] and DENV $NS3_{256\text{-}265}$ [ACK57817.1]), yellow fever virus (YFV) (VIDAMCHATL: YFV $NS3_{255\text{-}264}$ [AIZ07887.1]) and West Nile virus (WNV) and Japanese encephalitis viruses (JEV) (IVDVMCHATL: both WNV $NS3_{255\text{-}264}$ [AFI56984.1] and JEV $NS3_{255\text{-}264}$ [ABU94628.1]. We used these peptides to load 721.174 cells and demonstrated that at 200μM in flow cytometry assays these peptides induced binding to KIR2DS2-tetramers, with enhanced binding of KIR2DS2 by the ZIKV and DENV peptide, IVDLMCHATF (**Fig. 5A**).

Our binding and functional experiments all used the KIR2DS2*001 allele and we therefore tested if allelic diversity of KIR affected KIR2DS2-mediated peptide recognition. We tested the alleles KIR2DS2*007 and KIR2DS*008, which have polymorphisms in the ligand binding domains compared to KIR2DS2*001 (*27*). Using a tetramer binding assay we found that these allelic variants had a similar peptide specificity as KIR2DS2*001 (**Fig. S5**). Thus allelic

diversity of KIR2DS2 did not influence recognition of HLA-C*0102 presented peptides by KIR2DS2.

To test if these flaviviral peptides could activate NK cells we tested Vav1 phosphorylation in NKL-2DS2 cells. 721.1.74 were loaded with peptide and co-cultured with NKL-2DS2 cells. The flaviviral peptides that bound KIR2DS2 also induced Vav1 phosphorylation in NKL-2DS2 cells (**Fig. 5B**). We next generated a 721.221 transfectant stably expressing HLA-C*0102 and the DENV/ZIKV peptide IVDLMCHATF. We co-cultured these cells with NKL, NKL-2DL2 and NKL-2DS2 cells. Endogenous expression of IVDLMCHATF with HLA-C*0102 resulted in augmented lysis of 721.221 transfectants by NKL-2DS2 as compared to lysis of 721.221 expressing HLA-C*0102 alone, but did not augment lysis by NKL or NKL-2DL2 cells (**Fig. 5C**).

To test the potential for KIR2DS2 to recognize native dengue virus we used a dengue replicon system (*28*). The DENV genome replicates at a slightly lower level in human embryonic kidney (HEK) cells expressing the replicon than during a wild-type virus infection, but with a slight overexpression of protein over time (**Fig. S6**). HEK cells stably expressing the dengue replicon were transiently transfected with HLA-C*0102 or HLA-C*0304. NKL-2DS2 preferentially lysed DENV replicating HEK cells transfected with HLA-C*0102 as compared to HEK:HLA-C*0102 not expressing DENV, and also HEK cells expressing both DENV and HLA-C*0102 cells as compared to those just expressing DENV (**Fig. 5D, 5E** and **Fig. S7**). However, we did not observe KIR2DS2-specific lysis of HEK cells expressing DENV and HLA-C*0304 (**Fig. 5F**). Thus in addition to HCV, KIR2DS2 also recognizes flavivirus helicase peptides in the context of HLA-C*0102.

Analysis of the crystal structures of the NS3 helicases of both HCV and DENV complexed with nucleic acids representative of the viral RNA indicate that similar to the HCV LNP epitope, the IVDLMCHATF peptide directly contacts the viral nucleic acid (**Fig. 5G**). Furthermore the NS3 helicases of DENV, ZIKV and JEV are all highly conserved, with this peptide occupying a similar position in all crystal structures (*25, 29-31*). Thus KIR2DS2 recognizes highly conserved peptide motifs, within the helicases of the *Flaviviridae*, which are directly involved in RNA binding and under extreme constraints on their ability to mutate.

Discussion

These data demonstrate that KIR2DS2 functions as an antigen specific receptor that recognizes conserved peptides from the *Flaviviridae* family of viruses. We have shown that KIR2DS2 recognizes: a peptide derived from the helicase 1a region of HCV, which is highly conserved amongst HCV genotypes; and also a conserved peptide sequence from flaviviruses, including the dengue and Zika viruses. The peptides are all have alanine and threonine at the the C-terminus -1 and -2 positions respectively, and within the flaviviral sequences, these two amino acids form part of an MCHAT motif within the helicase 1b region and which is conserved in 61 out of 63 flaviviruses. The peptides can be endogenously present by HLA-C*0102, and the combination of the HCV peptide LNPSVAATL and HLA-C*0102 is sufficient for KIR2DS2 to inhibit replication *in vitro*. Thus KIR2DS2 has some functions analogous to a T cell receptor in recognizing peptide:MHC, but has a broad specificity in that is also recognizes HLA-C*0304 and peptide (*12*). Binding to different peptides derived from pathogens, and also different HLA class I molecules is a likely pre-requisite for KIR2DS2 to have reached its current population frequency of approximately 50%. Our experiments suggest that an additional HCV peptide may be presented by HLA-C*0304 to KIR2DS2. However, further work is required to define the complete specificity of this receptor.

A broad specificity for KIR2DS2 is consistent with our understanding of how inhibitory KIR engage HLA class I (*10*). The recognition of different peptides and HLA class I allotypes is facilitated by the motif-based recognition of HLA class I by KIR, in which the KIR:HLA interface is stabilized by salt bridges (*32*) and peptide selectivity is determined by the C-terminus -1 and -2 residues of the peptide. Thus although the HCV and DENV peptides share only 2 residues, both are recognized by KIR2DS2 in the context of the same HLA class I molecule. This is consistent with the mode of binding observed for the HLA-C specific

inhibitory KIR. KIR2DS2 thus demonstrates similarities in binding properties to the inhibitory KIR, but with distinct peptide selectivity from its inhibitory counterparts, KIR2DL2 and KIR2DL3. One concern is that a broad peptide specificity may lead to autoreactivity and interestingly, there is an association of KIR2DS2 with the autoimmune disease systemic sclerosis and rheumatoid vasculitis (*33, 34*).

We have studied ligands for KIR2DS2 *in vitro*, and analysis of our HCV population demonstrated an *in vivo* correlation of KIR2DS2 with the outcome of HCV infection. However, to date there are no studies that demonstrate an *in vivo* role for KIR2DS2 in flavivirial infection. In an immunogenetic study there was an under-representation of KIR2DS2 in dengue virus (39.0%) infected individuals as compared to healthy controls (64.8%) (*35*), suggesting a positive association of KIR2DS2 with dengue virus clearance. Furthermore, during acute dengue virus infection NK cells are activated *in vivo*, but testing of KIR2DS2-positive NK cells in this context is difficult because of the lack of specific reagents that distinguish KIR2DS2 from KIR2DL2/3. Thus further *in vivo* work is required to determine whether KIR2DS2-positive NK cells are specifically activated during acute flaviviral infections.

Nonetheless higher KIR2DS2 gene frequencies are seen in populations from Central and Southern Africa where flaviviral infections are more common (*36*). Furthermore, within the Amerindian population both the A and the B KIR haplotypes have been maintained (*37*). This balancing selection is thought to be due to the combined effects of the KIR B haplotype protecting against pregnancy induced disease and the KIR A haplotype protecting against infectious disease. However, the genes associated with protection against pregnancy associated diseases are located in the telomeric end of the KIR locus, and so our data are consistent with a model in which the population frequency of the centromeric end of the B

haplotype is maintained through protection against infectious disease. A broad specificity of KIR2DS2 for different HLA-C allotypes complexed with peptides derived from pathogenic virus, provides a rationale for the evolution of this family of receptors. Our observations, coupled with the recent discoveries of adaptive properties of NK cells, make them potential targets for novel therapeutic strategies against flaviviral infections.

Materials and methods

Patients

The cohort of HCV-exposed individuals was recruited from UK hepatology clinics (*4, 38*). Two hundred and thirty-three subjects had chronic HCV infection, and 128 had resolved infection. Overall 239 (69%) were male, and 289 (82%) had acquired HCV through intravenous drug usage.

HCV replicon

The N17/JFH1 subgenomic replicon encoding the firefly luciferase reporter and the puromycin resistance marker has been described previously (*21*). Site-directed mutagenesis was performed using the QuikChange-XL-II kit (Agilent Technologies, Santa Clara, CA) with appropriate primers (sequences available upon request). The N17 replicon RNAs were generated *in vitro* using the T7 Megascript kit (Applied Biosystems, Paisley, UK). To measure replication of N17 SGR/JFH1WT, 4×10^6 naive HUH7 cells were electroporated with 10 µg of viral RNA, cells were seeded in triplicate, lysed and luciferase activity measured using the Bright-Glo Luciferase assay system (Promega, Madison, WI). HUH7 cells electroporated with the WT or the L9D variant of the N17 replicon RNA were cultured in the presence of 2 *µ*g/ml puromycin (Life Technologies, Paisley, U.K.) and the surviving cells were pooled and established as stable replicon-expressing cell lines.

Cell lines and transfectants

721.174 and HUH7 cells were cultured in R10 medium (RPMI medium 1640 supplemented with 1% penicillin streptomycin [Life Technologies]) or DMEM and 10% FCS (Lonza, Slough, U.K.). HLA-C*0102 or HLA-C*0304 were cloned into the pIB vector (*39*) and transfected into the HUH7.5 cells. The HEK:DENV replicon cells were grown in DMEM and 10% FCS supplemented with 2µg/mL puromycin. The HLA-C*0304:ICP47 cell line was made by

transfecting 721.221:C*0304 cells with the ICP47 gene cloned into pCDNA 3.1 using the Polyplus jetPRIME® transfection system (SourceBioScience, Nottingham, UK) and selected using hygromicin 500*μ*g/mL (Invivogen, CA). The NKL cell line was transfected with the KIR2DL2, KIR2DS2 or KIR2DL3 cloned into the pIB vector as previously described.

HUH7 cell lines stably expressing the WT N17 replicon or the L9D variant described above were transduced with pIB-HLA-C*0102 expressing lentiviral vector. The transduced cells were selected with 2μg/mL puromycin and 1 to 6μg/mL blasticidin. HUH7:C*0102:replicon cells were co-cultured with NKL cell lines for 24 hours at various E:T ratios for 24 hours, and then luciferase activity assessed.

NK cell assays

*CD107a degranulation***.** PBMCs were stimulated overnight with 1ng/mL rHuIL-15 (R&D Systems, Abingdon, U.K.) Peptides were synthesized by GL Biochem Ltd (Shanghai, China) or Peptide Protein Research (Fareham, U.K.). 721.174 cells were incubated with peptide at 26°C overnight, washed, resuspended with the PBMCs at an E:T ratio of 5:1 and anti–CD107a-AF647 (20μL/mL). Cells were then incubated at 26°C for 4hrs with 6μg/mL Golgi-Stop (BD Biosciences, Oxford, U.K.) added after 1hr prior to staining and analysis by flow cytometry

Cell tracker Orange (CTO) cytotoxicity assays. 721.174 cells were incubated with peptide at 26 °C for 16hrs, then with CellTracker™ Orange CMTMR (Life Technologies) and resuspended with NK cell clones at an E:T ratio of 10:1. Co-cultures were incubated at 26°C for 4h, stained with Live/Dead fixable Aqua dead cell stain (Life Technologies) and fixed in 1% (w/v) PFA prior to analysis by flow cytometry.

LNP construct. A construct expressing HLA-C*0102 in continuity with the 2A self-cleaving peptide sequence from Thosea asigna virus the E3/19K ER-targeting sequence and the

LNPSVAATL or IVDLMACHATF peptide was synthesized from Gene Art™ (Life Technologies), cloned into the pIB vector and transduced into the 721.221 cell line.

Inhibition of HCV replication assays. Target cells Huh7-J17-WT/HLA and Huh7-J17-R1/HLA were seeded. The next day, NKLs were co-cultured with the target cells in duplicate for 24 hr. Plates were then centrifuged and the cell pellet lysed with Glo Lysis Buffer (Promega). 50μl of each lysate was read using 50 μl of luciferase assay reagent Promega) on a GloMax® Discover Luminometer.

HEK Cell Cytotoxic Killing Assay. HEK and HEK:DENV cells were transiently transfected with 2ug of C*0102mCherry-pCDNA3 or C*0304mCherry-pCDNA3 using Polyplus jetPrime (SourceBioscience, UK). After 24 hours cells were co-cultured for 24 hours with NKL cell lines in triplicate at an E:T ratio of 6:1. Cells were stained with Live/Dead Zombie Violet stain (BioLegend, UK) for one hour, fixed with 1% paraformaldehyde-PBS solution and analyzed by flow cytometry. DENV-positive HEK cells were detected by the GFP expression of the DENV construct, and HLA-C*0102, or HLA-C*0304, transfected cell lines by mCherry expression. The percentage cytotoxicity was determined by calculating: the percentage of zombie violet positive cells in the presence of effectors minus the percentage of zombie violet positive cells in the absence of effectors.

KIR staining

The extracellular domain of KIR2DS2*001 or KIR2DL2*001 containing a C terminal biotinylation tag was cloned into pET23d+ vector. This was expressed as inclusion bodies in Rosetta^{TM}2 (DE3) bacteria (MerckMillipore, Feltham, U.K.), purified, denatured and reduced in 6M guanidine-HCL and 20mM DTT. KIR2DS2 was purified by gel filtration chromatography using FPLC. Biotinylation was performed using a BirA biotinylation kit (Avidity, Aurora, CO). Fluorescently-labeled tetramers were produced by coupling biotinylated KIR2DS2 molecules to PE-conjugated streptavidin (Molecular Probes^{TM}, Life Technologies). The KIR2DS2*007

and KIR2DS2*008 tetramers were made from a KIR2DS2*001 template using the QuikChange Lightening Site-Directed Mutagenesis Kit (Agilent Technologies, Cheshire, UK), (primer sequences are available on request). The KIR2DL2-IgG fusion construct (KIR2DL2-Fc Chimera; R&D Systems Inc., Minneapolis, MN) was conjugated with protein A Alexa Fluor 488 (Life Technologies).

KIR genotyping

KIR genotyping of the donors was performed by qPCR as previously described (*4*).

NK cell clones

NK cells ($CD3^-$ $CD56^+$ $CD158b^+$) were single cell sorted from PBMC from a *KIR2DL2*$^+$*S2*$^+$*L3*$^-$ donor into SCGM media (CellGenix, Freiburg, Germany) containing 5% heat-inactivated human serum and IL-12 (10 ng/mL) (Peprotech, NJ,), IL-15 (20 ng/mL) and IL-18 (100 ng/mL) (both R&D Systems). Clones were fed weekly with irradiated PBMC (1 x 10^6/mL), 250iu/ml IL-2 were and 2.5 µg/mL PHA (Fischer Scientific, Loughborough, U.K.). Clones were typed for expression of *KIR2DS2* by RT-qPCR. RNA was extracted from the NK clones using TRIzol® (Life Technologies), reverse transcribed using a high capacity reverse transcriptase kit (Applied Biosystems). 1ng of cDNA was used for qPCR analysis. *KIR2DS2, KIR2DL2, KIR2DL3* primers and probes were as described described (*40*). Each sample was read in triplicate and gene expression was determined using the ΔCt method.

Conjugate formation and staining

721.174 cells were incubated overnight at 26°C in the absence or presence of 100µM peptide. 1 x 10^5 Ba/F3-KIR2DS2 or Ba/F3-KIR2DL2 cells (a gift from Dr Lewis Lanier) were co-incubated with the 721.174 cells at an E:T ratio of 2:1. Cells were fixed in 4% (w/v) PFA in PBS and then stained with 20 µg/mL CD158b-PE (GL183) antibody (Beckmann Coulter,

High Wycombe, U.K.). Cells were imaged using a Leica SP5 resonance scanning microscope (Leica Microsystems, Milton Keynes, U.K.). Transmission images and PE emission were collected in different channels. Data were processed using Leica Imaging software and ImageJ software (http://imagej.nih.gov/ij).

Immunoprecipitation and Western blotting

721.174 cells were cultured with 20mM peptide overnight at 26°C. NKL-2DS2 and 721.174 cells were coincubated at a 1:1 E:T ratio for 5 min at 37°C and lysed in 20mM Tris-HCl, pH7.6; 150mM NaCl; 1mM EDTA; 1mM sodium orthovanadate; and 0.5%Triton X-100. KIR were immunoprecipitated with anti-CD158b (clone GL183; AbD Serotec, Oxford, U.K.) and analyzed by Western blotting. Abs recognizing phospho-Vav1 (EP510Y; Abcam, Cambridge, U.K.), Vav1 (Cell Signaling Technology, Hitchin, U.K.), anti-phosphotyrosine (4G10 Platinum, Millipore), DAP-12 (clone D7G1X; Cell Signaling Technology), were used with HRP conjugated secondary Abs (Cell Signaling Technology, Hitchin, U.K.). Membranes were stripped using the Western blot Recycling Kit (Alpha Diagnostics, San Antonio, TX). Protein bands were detected by chemiluminescence (SuperSignal West Pico Chemiluminescent Substrate; Perbio Science, Cramlington, U.K.), using the ChemiDoc-It Imaging System with VisionWorks software (UVP), and quantified with ImageJ software.

Peptide binding analysis

The online resources ADT, Net-MHC pan and KISS were used to search for potential HLA-C*0102 binding epitopes (*41-43*).

Statistical Analysis

Statistical analyses (t-tests and ANOVA) were performed using GraphPad Prism®, version 6 (La Jolla, CA) and logistic regression analysis performed using SPSS V20.0 (IBM, Armonk, NY).

Supplementary materials

Figure S1: Peptide stabilization of HLA-C*0102 by HCV peptides

Figure S2: The effect of single HCV peptides on degranulation of CD158b NK cells

Figure S3: Cytotoxicity of KIR2DS2+ NK cell clones to peptide loaded 721.174 cells

Figure S4: KIR2DS2-tetramer binding to HLA-C*0102 and HCV peptides or VAPWNSLSL peptide derivatives

Figure S5: Flow cytometry plots comparing binding of KIR2DS2*001, KIR2DS2*007 and KIR2DS2*008 binding to HLA-C*0102 and peptide

Figure S6: Analysis of viral RNA and protein production in DENV replicon containing cells compared to DENV-2 infected cells.

Figure S7: Flow cytometry plots illustrating gating strategy and killing of HEK cells expressing GFP-tagged Dengue virus replicon by NKL-2DS2 cells

Table S1: Summary of hepatitis C virus (HCV) peptides identified to bind HLA-C*0102

Table S2: Protein sequence alignment of hepatitis C viruses

Table S3: Flavivirus NS3 HLA-C*0102 binding peptides as determined by NetMHCpan.

Table S4: Accession numbers of *Flavivirus* sequences used to compile the alignment in Figure 4

Data file S1: Raw data for Figures 1-5

Data file S2: Western blot gels for Figures 1-5

References and notes

1. G. Alter *et al.*, HIV-1 adaptation to NK-cell-mediated immune pressure. *Nature* **476**, 96-100 (2011).
2. C. Petitdemange *et al.*, Unconventional repertoire profile is imprinted during acute chikungunya infection for natural killer cells polarization toward cytotoxicity. *PLoS Pathog* **7**, e1002268 (2011).
3. E. Townsley *et al.*, Interaction of a dengue virus NS1-derived peptide with the inhibitory receptor KIR3DL1 on natural killer cells. *Clin Exp Immunol* **183**, 419-430 (2016).
4. S. I. Khakoo *et al.*, HLA and NK cell inhibitory receptor genes in resolving hepatitis C virus infection. *Science* **305**, 872-874 (2004).
5. M. P. Martin, M. Carrington, Immunogenetics of HIV disease. *Immunol Rev* **254**, 245-264 (2013).
6. G. B. Cohen *et al.*, The selective downregulation of class I major histocompatibility complex proteins by HIV-1 protects HIV-infected cells from NK cells. *Immunity* **10**, 661-671. (1999).
7. W. F. Garcia-Beltran *et al.*, Open conformers of HLA-F are high-affinity ligands of the activating NK-cell receptor KIR3DS1. *Nat. Immunol.*, (2016).
8. M. A. Ivarsson, J. Michaelsson, C. Fauriat, Activating killer cell Ig-like receptors in health and disease. *Frontiers in immunology* **5**, 184 (2014).
9. L. Fadda *et al.*, Peptide antagonism as a mechanism for NK cell activation. *Proc. Natl. Acad. Sci. U. S. A.* **107**, 10160-10165 (2010).
10. M. J. Sim *et al.*, Canonical and Cross-reactive Binding of NK Cell Inhibitory Receptors to HLA-C Allotypes Is Dictated by Peptides Bound to HLA-C. *Frontiers in immunology* **8**, 193 (2017).

11. X. Saulquin, L. N. Gastinel, E. Vivier, Crystal structure of the human natural killer cell activating receptor KIR2DS2 (CD158j). *J. Exp. Med.* **197**, 933-938 (2003).

12. C. A. Stewart *et al.*, Recognition of peptide-MHC class I complexes by activating killer immunoglobulin-like receptors. *Proc. Natl. Acad. Sci. U. S. A.* **102**, 13224-13229 (2005).

13. J. Liu, Z. Xiao, H. L. Ko, M. Shen, E. C. Ren, Activating killer cell immunoglobulin-like receptor 2DS2 binds to HLA-A*11. *Proc. Natl. Acad. Sci. U. S. A.* **111**, 2662-2667 (2014).

14. T. Graef *et al.*, KIR2DS4 is a product of gene conversion with KIR3DL2 that introduced specificity for HLA-A*11 while diminishing avidity for HLA-C. *J. Exp. Med.* **206**, 2557-2572 (2009).

15. L. Thiruchelvam-Kyle *et al.*, The Activating Human NK Cell Receptor KIR2DS2 Recognizes a beta2-Microglobulin-Independent Ligand on Cancer Cells. *J. Immunol.* **198**, 2556-2567 (2017).

16. C. L. Thio *et al.*, HLA-Cw*04 and hepatitis C virus persistence. *J. Virol.* **76**, 4792-4797 (2002).

17. L. D. Barber *et al.*, The inter-locus recombinant HLA-B*4601 has high selectivity in peptide binding and functions characteristic of HLA-C. *J. Exp. Med.* **184**, 735-740. (1996).

18. R. DeMars *et al.*, Mutations that impair a posttranscriptional step in expression of HLA-A and -B antigens. *Proc. Natl. Acad. Sci. U. S. A.* **82**, 8183-8187 (1985).

19. S. Cassidy *et al.*, Peptide selectivity discriminates NK cells from KIR2DL2- and KIR2DL3-positive individuals. *Eur. J. Immunol.*, (2014).

20. L. L. Lanier, B. C. Corliss, J. Wu, C. Leong, J. H. Phillips, Immunoreceptor DAP12 bearing a tyrosine-based activation motif is involved in activating NK cells. *Nature* **391**, 703-707 (1998).

21. A. G. Angus *et al.*, Conserved glycine 33 residue in flexible domain I of hepatitis C virus core protein is critical for virus infectivity. *J. Virol.* **86**, 679-690 (2012).

22. K. Kurokohchi *et al.*, Expression of HLA class I molecules and the transporter associated with antigen processing in hepatocellular carcinoma. *Hepatology* **23**, 1181-1188 (1996).

23. A. G. Angus *et al.*, Requirement of cellular DDX3 for hepatitis C virus replication is unrelated to its interaction with the viral core protein. *J Gen Virol* **91**, 122-132 (2010).

24. J. C. Boyington, A. G. Brooks, P. D. Sun, Structure of killer cell immunoglobulin-like receptors and their recognition of the class I MHC molecules. *Immunol Rev* **181**, 66-78. (2001).

25. M. Gu, C. M. Rice, Three conformational snapshots of the hepatitis C virus NS3 helicase reveal a ratchet translocation mechanism. *Proc. Natl. Acad. Sci. U. S. A.* **107**, 521-528 (2010).

26. D. Luo, S. G. Vasudevan, J. Lescar, The flavivirus NS2B-NS3 protease-helicase as a target for antiviral drug development. *Antiviral Res* **118**, 148-158 (2015).

27. J. Robinson, J. A. Halliwell, H. McWilliam, R. Lopez, S. G. Marsh, IPD--the Immuno Polymorphism Database. *Nucleic Acids Res* **41**, D1234-1240 (2013).

28. N. Masse *et al.*, Dengue virus replicons: production of an interserotypic chimera and cell lines from different species, and establishment of a cell-based fluorescent assay to screen inhibitors, validated by the evaluation of ribavirin's activity. *Antiviral Res* **86**, 296-305 (2010).

29. D. Luo *et al.*, Insights into RNA unwinding and ATP hydrolysis by the flavivirus NS3 protein. *EMBO J* **27**, 3209-3219 (2008).

30. R. Jain, J. Coloma, A. Garcia-Sastre, A. K. Aggarwal, Structure of the NS3 helicase from Zika virus. *Nat Struct Mol Biol*, (2016).

31. T. Yamashita *et al.*, Crystal structure of the catalytic domain of Japanese encephalitis virus NS3 helicase/nucleoside triphosphatase at a resolution of 1.8 A. *Virology* **373**, 426-436 (2008).

32. J. C. Boyington, P. D. Sun, A structural perspective on MHC class I recognition by killer cell immunoglobulin-like receptors. *Mol Immunol* **38**, 1007-1021. (2002).

33. T. Momot *et al.*, Association of killer cell immunoglobulin-like receptors with scleroderma. *Arthritis Rheum* **50**, 1561-1565 (2004).

34. J. H. Yen *et al.*, Major histocompatibility complex class I-recognizing receptors are disease risk genes in rheumatoid arthritis. *J. Exp. Med.* **193**, 1159-1167. (2001).

35. C. Petitdemange *et al.*, Association of HLA class-I and inhibitory KIR genotypes in Gabonese patients infected by Chikungunya or Dengue type-2 viruses. *PLoS One* **9**, e108798 (2014).

36. F. F. Gonzalez-Galarza *et al.*, Allele frequency net 2015 update: new features for HLA epitopes, KIR and disease and HLA adverse drug reaction associations. *Nucleic Acids Res* **43**, D784-788 (2015).

37. K. Gendzekhadze *et al.*, Co-evolution of KIR2DL3 with HLA-C in a human population retaining minimal essential diversity of KIR and HLA class I ligands. *Proc. Natl. Acad. Sci. U. S. A.* **106**, 18692-18697 (2009).

38. S. Ashraf *et al.*, Synergism of tapasin and human leukocyte antigens in resolving hepatitis C virus infection. *Hepatology* **57**, 881-889 (2013).

39. G. Borhis *et al.*, A peptide antagonist disrupts NK cell inhibitory synapse formation. *J. Immunol.* **190**, 2924-2930 (2013).

40. S. Cooley *et al.*, A subpopulation of human peripheral blood NK cells that lacks inhibitory receptors for self-MHC is developmentally immature. *Blood* **110**, 578-586 (2007).

41. I. Hoof *et al.*, NetMHCpan, a method for MHC class I binding prediction beyond humans. *Immunogenetics* **61**, 1-13 (2009).

42. L. Jacob, J. P. Vert, Efficient peptide-MHC-I binding prediction for alleles with few known binders. *Bioinformatics* **24**, 358-366 (2008).

43. N. Jojic, M. Reyes-Gomez, D. Heckerman, C. Kadie, O. Schueler-Furman, Learning MHC I--peptide binding. *Bioinformatics* **22**, e227-235 (2006).

Acknowledgements:

This work was supported by grants from The Wellcome Trust WT089883MA (SAC) WT093465MA (MP) and WT076991MA (SIK); and the MRC G1001738 (SIK), G0401586 (AD) and MC_UU 12014/2 (AHP). We would like to thank L Lanier for reagents, S Gadola, L Tereza, J Vivian for helpful discussions and A Al-Shamkhani for critical reading of the manuscript.

Author Contributions:

MMN, SAC, AM, VC, CK, BM, SM AHP, MAP SIK designed experiments, MMN, SAC, AM, VC, CK, BM, SM, PR performed experiments; ADD, AM, LJF, FHJC, CR provided key reagents; MMN, AHP, MAP, ADD and SIK wrote the manuscript; MMN, SAC, CK and SIK performed data analysis, MMN, SAC, CK, SH and SIK performed statistical analysis.

Competing interests

SIK, MMN, MP have applied for a patent on the use of peptides for NK cell therapy

Figure 1

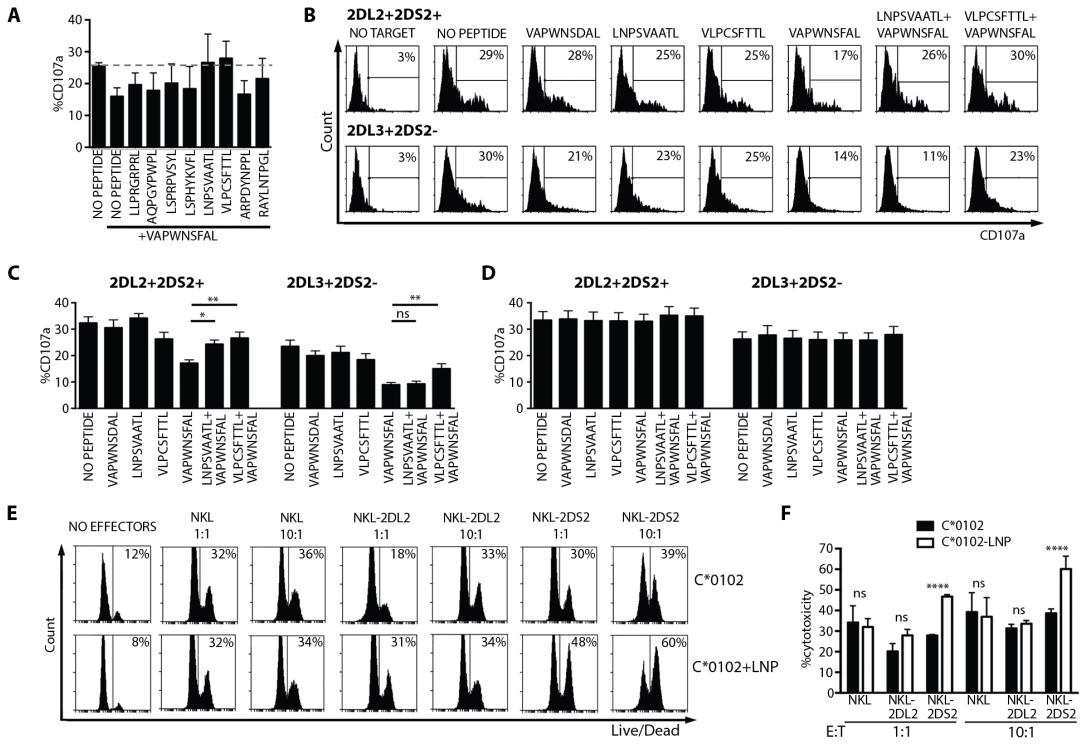

Figure 1. KIR2DS2 recognizes the HCV peptide LNPSVAATL

1A PBMC were stimulated overnight with IL-15, and incubated for four hours with 721.174 cells that had been loaded with VAPWNSFAL or with VAPWNSFAL plus the indicated HCV peptides at concentration of 5μM. The mean CD107a expression plus one standard error on $CD3^{-}CD56^{+}CD158b^{+}$ NK cells from three unselected donors is shown. **1B-D** CD107a degranulation assays of NK cells from *KIR2DL2*$^{+}$*/KIR2DS2*$^{+}$ and *KIR2DL3*$^{+}$*/KIR2DS2*$^{-}$ donors in response to 721.174 cells incubated with indicated peptides. Peptides were used at 5μM each. **1B** shows flow cytometry histogram plots of CD107a expression gated on $CD3^{-}$ $CD56^{+}CD158b^{+}$ NK cells from two donors of different KIR genotype. The results from five donors of each genotype are summarized for $CD158b^{+}$ NK cells in (**1C**) and for $CD158b^{-}$ NK cells in (**1D**). Means and standard errors for each condition are shown. P values indicate comparison to VAPWNSFAL alone. **1E,F** NKL cells either untransfected or transfected with

KIR2DL2 or KIR2DS2 were incubated with 721.221 cells transfected with HLA-C*0102 or with HLA-C*0102+LNPSVAATL (C*0102-LNP) and the cytotoxicity of the 721.221 cells measured by flow cytometry. **1D** shows flow cytometry histogram plots of the uptake of the Live/Dead fixable aqua dead dye by the target cells incubated with the indicated effector cells (**1E**). The means and standard errors from three independent cytotoxicity experiments are shown in (**1F**). Effector to target (E:T) ratios are also shown. P values indicate the comparison of cytotoxicity between the HLA-C*0102 and the HLA-C*0102-LNP targets. Where shown p values were determined by independent two-tailed t-tests (*$p<0.05$, **$p<0.01$,***$p<0.001$).

Figure 2

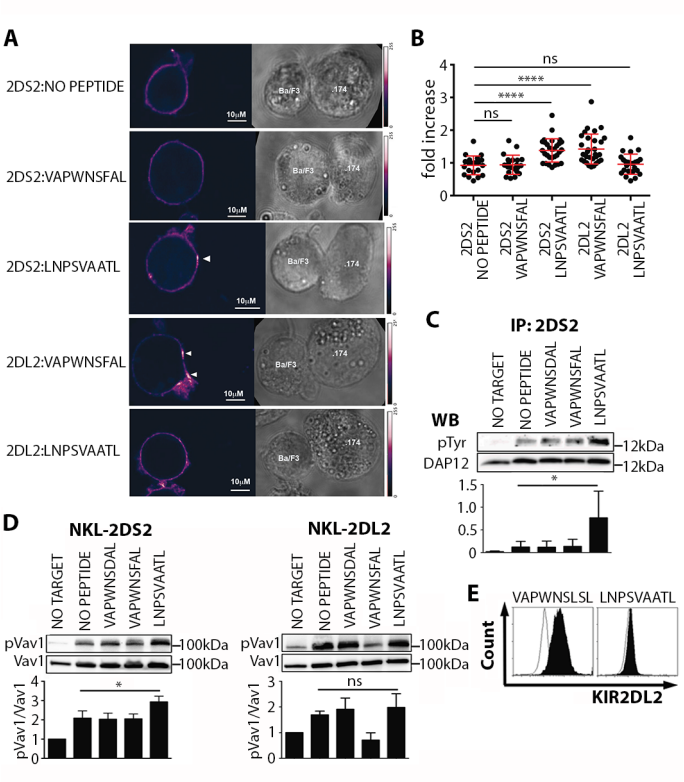

Figure 2. LNPSVAATL activates KIR2DS2-postiive, but not KIR2DL2-positive, NK cells

2A,B Ba/F3 cells expressing KIR2DS2 or KIR2DL2 were incubated with 721.174 cells loaded the indicated peptides. Cells were fixed and stained with anti-CD158b prior to analysis by confocal microscopy (**2A**). Peptides were used at a concentration of 100µM. Arrows indicate clustering at the interface between the cells Ba/F3 and 721.174 cells. The intensity of staining of the Ba/F3 cell at the interface was compared with the membrane at a non-contact area, and plotted as the fold increase above background (**2B**). The results from three independent experiments with a total of thirty conjugates per condition is shown. The p value in comparison to 2DS2 with no peptide is shown. **2C** NKL-2DS2 cells were incubated with 721.174 cells loaded with the indicated peptides and DAP12 was co-immunoprecipitated with anti-2DS2 antibody from the cell lysates prior to Western blot with anti-phosphotyrosine (pTyr) or anti-DAP12. DAP12 was also immunoprecipitated from NKL-2DS2 cells in the absence of 721.174 target cells (no target). Densitometry results of the pDAP12/DAP12 ratio

from three independent experiments and p values in comparison to no peptide are shown. **2D** NKL-2DS2 or NKL-2DL2 cells were incubated with 721.174 cells loaded with the indicated peptides and Western blotting for phospho-Vav1 (pVAv1) or Vav1 performed. "No target" lanes indicate immunoprecipitation from NKL-2DS2 or NKL-2DL2 cells alone. Densitometry results of the phospho-Vav1/Vav1 ratio from three independent experiments and p values in comparison to no peptide are shown. **2E** 721.174 cells were cultured with 100μM peptide (VAWPNSLSL or LNPSVAATL) overnight then stained with the KIR2DL2-Fc fusion construct and analyzed by flow cytometry. Shown are the histogram plots for the two peptides (filled histograms) and the median fluorescence of KIR2DL2-Fc, compared with no peptide (open histograms). For all panels p values were derived using one-way ANOVA with Dunnett's test for multiple comparisons **(***$p<0.05$, ****$p<0.0001$).

Figure 3

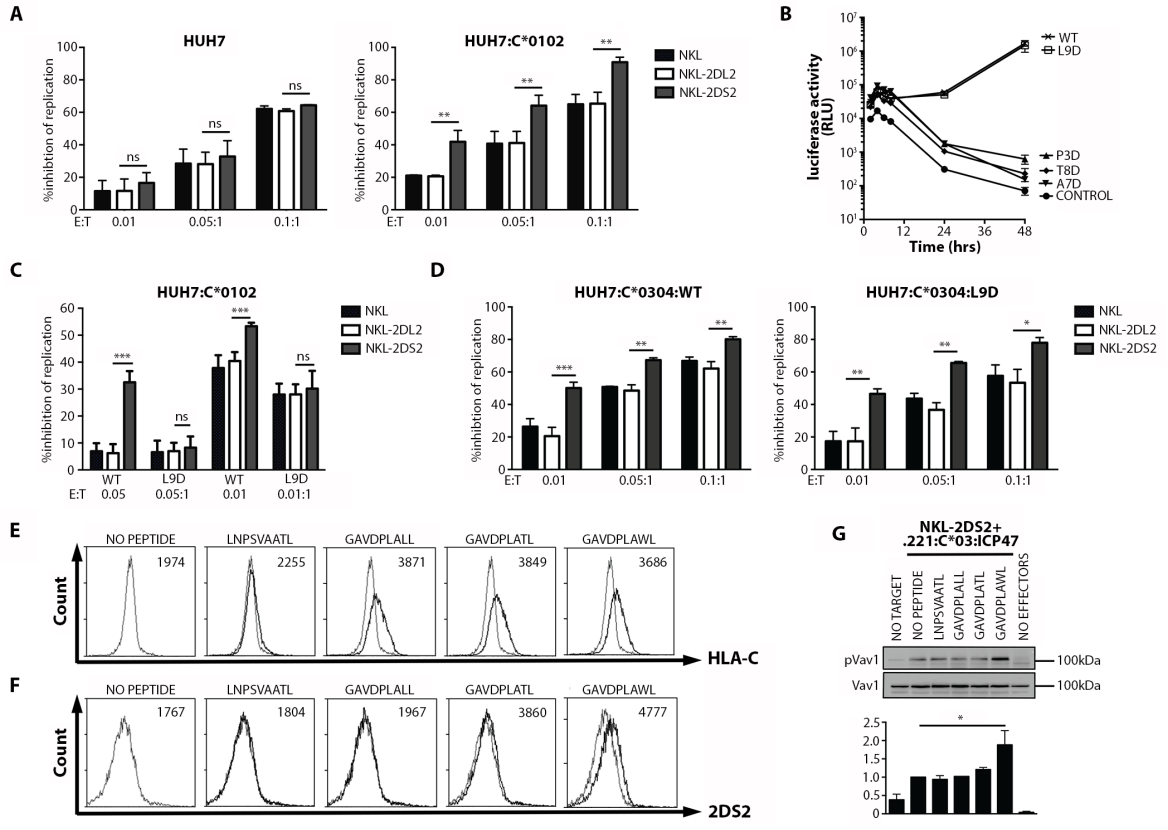

Figure 3. Endogenously presented LNPSVAATL is recognized by KIR2DS2 in the context of HCV

3A HUH7 cells expressing the N17 (JFH1ΔE1E2-luc) replicon with (right panel) or without (left panel) HLA-C*0102 were co-incubated with NKL, NKL-2DL2 or NKL-2DS2 cells at the indicated E:T ratios. Luciferase activity from the co-cultures was measured and normalized to expression in the absence of NKL cells. The relative inhibition of replication was then measured. The means and standard errors of three experiments performed in duplicate are shown. Comparisons for NKL-2DS2 with NKL-2DL2 are indicated. **3B** Replication of wild type (WT) N17 (JFH1ΔE1E2-luc) replicon RNA, or variants in which the LNPSVAATL epitope had been mutated to aspartate at residues 3, 7, 8, 9 (P3D, A7D, T8D and L9D respectively). As a non-replicating control (Control), the N17 replicon carrying the lethal GND mutation in the viral NS5B protein was used. **3C** NKL, NKL-2DL2 or NKL-2DS2 cells were co-cultured

with HUH7-C*0102 cells expressing either wild-type (WT) or the L9D mutant HCV replicon. Luciferase activity was measured and plotted as percentage inhibition of viral RNA replication compared to HUH7 cells incubated in the absence of NKL cells. Shown are the means and standard errors of three experiments performed in duplicate and p values for comparisons between NKL-2DS2 and NKL-2DL2. **3D** NKL, NKL-2DL2 or NKL-2DS2 cells were co-cultured with HUH7-C*0304 cells expressing either wild-type (WT) (left panel) or the L9D mutant HCV replicon (right panel). The percentage inhibition of replication compared to the no NKL control is shown. Statistical analyses for **3A,C,D** were performed using independent two-tailed t-tests to compare NKL-2DS2 and NKL-2DL2. **3E, F** 721:C*0304:ICP47 cells were loaded with the indicated peptides at saturating concentrations (100μM) and then stained for HLA-C expression using the DT9 antibody (**3E**) or the KIR2DS2-PE tetramer (**3F**). One representative histogram plot from three independent experiments is shown for each peptide and the median fluorescence intensity of staining indicated. Dark lines indicate peptide staining compared to the no peptide control (gray lines). **3G** Western blot for phospho-Vav1 and Vav1 from 721.221:C*0304:ICP47 cells cultured with 20μM of the indicated peptide and co-incubated with NKL-2DS2 cells at a 1:1 E:T ratio. One representative blot is shown together with densitometry of the phospho-Vav1/Vav1 ratio (mean$\pm$SD) from three independent experiments. Statistical analysis was performed using one-way ANOVA with Dunnett's test for multiple comparisons (*$p<0.05$, **$p<0.01$,***$p<0.001$).

Figure 4

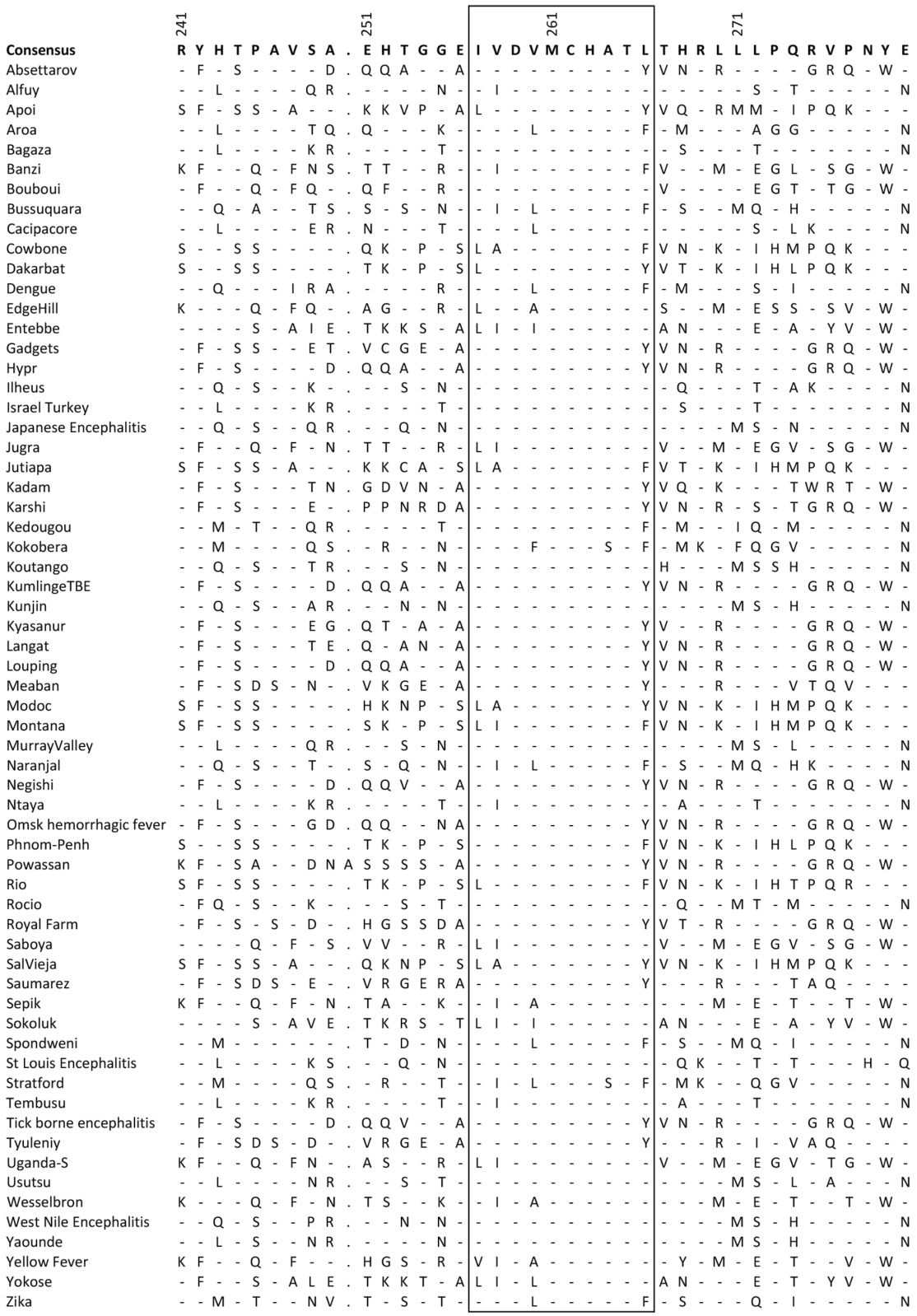

Figure 4: Protein sequence alignment of the NS3 helicase-encoding region of 63 *Flaviviruses* demonstrate conservation of a KIR2DS2-binding peptide

The box indicates the putative KIR2DS2 binding peptide. Numbering is from the start of the NS3 protein of Dengue virus.

Figure 5

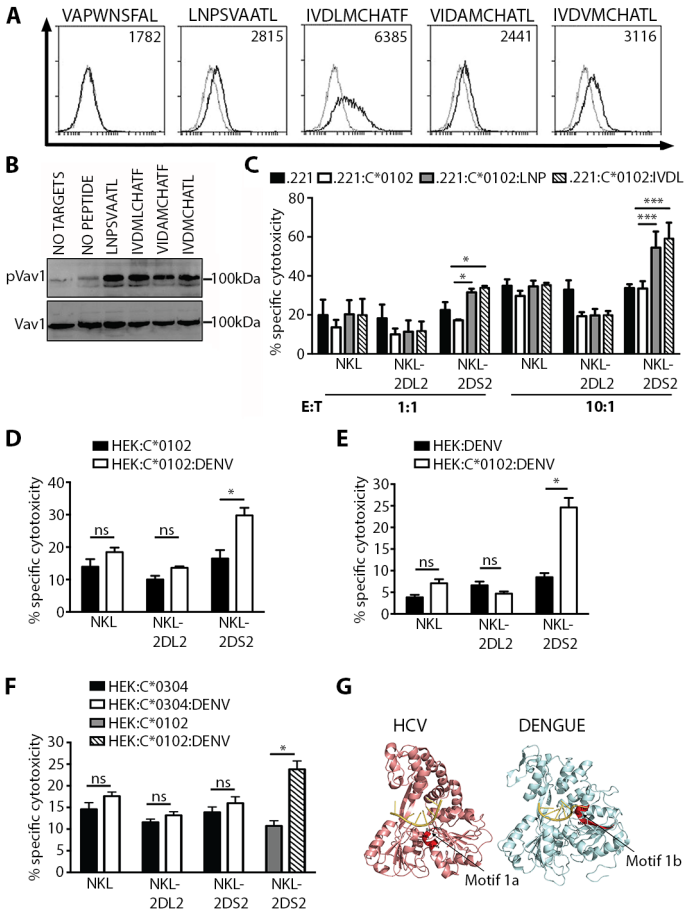

Figure 5. KIR2DS2 recognizes conserved helicase peptides from multiple flaviviruses

5A KIR2DS2 tetramer (black lines) binding to 721.174 cells incubated with the indicated peptides at saturating concentrations (200μM) as compared to no peptides (grey lines). The median fluorescence of tetramer staining of peptide is indicated (JEV:Japanese Encephalitis virus). **5B** NKL-2DS2 cells were incubated with 721.174 cells pre-loaded with the indicated Flavivirus peptides and then assayed for phospho-Vav1 and Vav1 by Western blotting. One representative blot of each is shown. **5C** The peptide IVDLMCHATF (IVDL) was co-expressed with HLA-C*0102 in 721.221 cells and used as targets in cytotoxicity assays in which effector cells were NKL, NKL-2DL2 and NKL-2DS2. Experiments were performed at an effector to target ratio of 6:1 and comparisons were made between the HLA-C*0102 transfectant and the HLA-C*0102:LNP or HLA-C*0102:IVDL cells. **5D-F** HEK, HEK-C*0102 or HEK:C*0304 cells expressing a dengue virus replicon (HEK:DENV, HEK:C*0102:DENV or

HEK:C*0304:DENV, respectively) or not were co-cultured with NKL cells expressing KIR2DS2 or KIR2DL2 and cytotoxicity assessed at 24 hours. The effect of dengue virus on KIR2DS2-mediated killing is shown in **5D** and the effect of HLA-C*0102 on KIR2DS2-mediated killing in **5E** and **Fig S5.** **5F** compares the effect of HLA-C*0304 on killing of DENV cells with that of HLA-C*0102 by NKL-2DS2. Means and standard errors of at least three independent experiments performed in triplicate are shown. **5G** Comparison of HCV (left panel) and Dengue NS3 helicases (right panel) showing contact of the LNPSVAATL (HCV) and IVDLMCHATF (Dengue) epitopes with the nucleic acid within the helicase domain (yellow). Selected amino acids from the epitopes are illustrated. Images were derived from structures published by Gu and Rice, and Luo *et al* and rendered using PyMOL (*25, 29*). Where shown p values were determined by independent two-tailed t tests (*$p<0.05$, ***$p<0.001$).

Table 1.

Genetic association of activating KIR with their putative ligands and the outcome of HCV infection in 336 individuals exposed to HCV (216 chronically infected and 120 with resolved HCV infection). Logistic regression was performed using SPSS v20.0 using the ENTER method. OR>1 indicates protection against chronic HCV infection.

	P	OR	95%CI
KIR2DL3/L3:HLA-C1/C1	0.005	2.68	1.34-5.37
KIR3DS1:HLA-B^{Bw4}	0.032	2.16	1.07-4.37
KIR2DS2:HLA-C1	0.033	2.06	1.06-4.02
KIR2DS3	0.033	0.51	0.27-0.95
KIR2DS1:HLA-C1	0.170	0.59	0.28-1.25
KIR2DS2:HLA-A*11	0.394	0.64	0.23-1.78
KIR2DS1:HLA-C2	0.509	0.74	0.31-1.80
KIR2DS2:HLA-C2	0.727	1.13	0.58-2.18

Supplementary materials

Figure S1: Peptide stabilization of HLA-C*0102 by HCV peptides

721.174 cells were incubated with the indicated peptides overnight at 26°C and then stained with the VP6G3 antibody and analyzed by flow cytometry. The median fluorescence intensity (MFI) was plotted at the different peptide concentrations. VAPWNSLSL is a naturally processed and presented self-peptide used as a positive control.

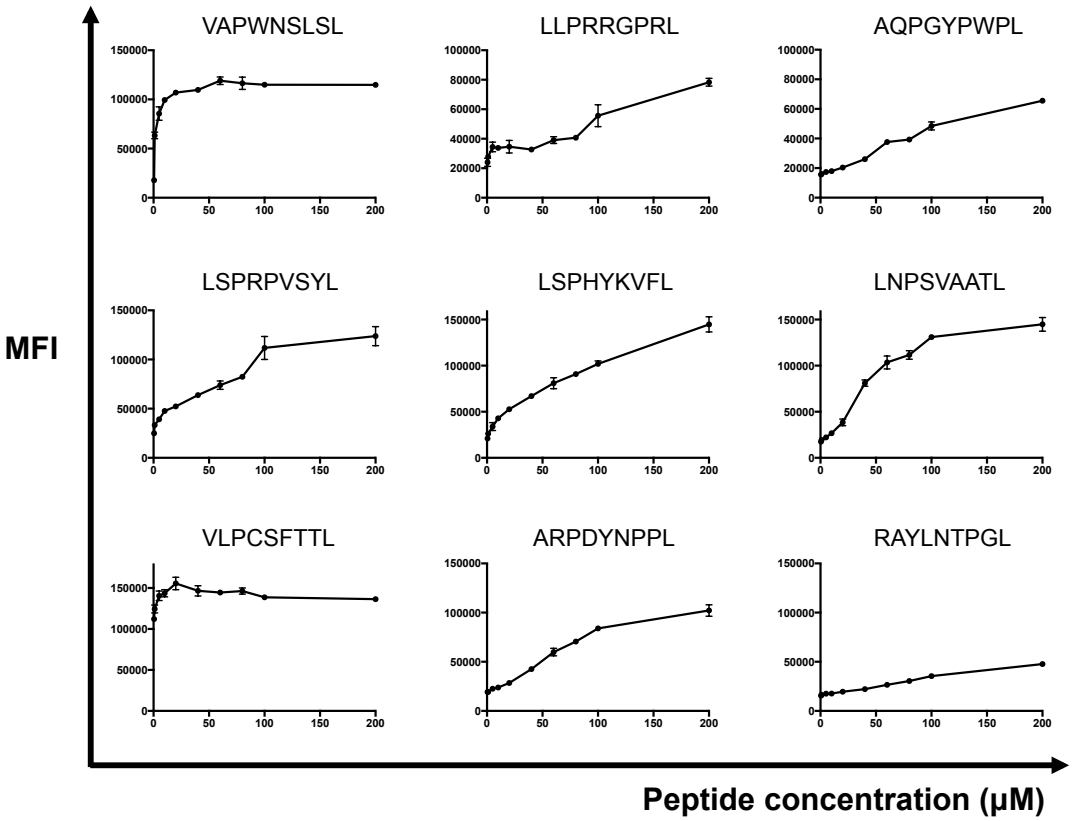

Figure S2: The effects of single HCV peptides on degranulation of CD158b NK cells: 721.174 cells were incubated with the indicated HCV peptides (100µM) and were then used as target cells in CD107a assays from NK cells from three unselected donors. Shown is the expression of CD107a on CD158b+ (KIR2DL2/L3/S2+) CD3-CD56+ NK cells.

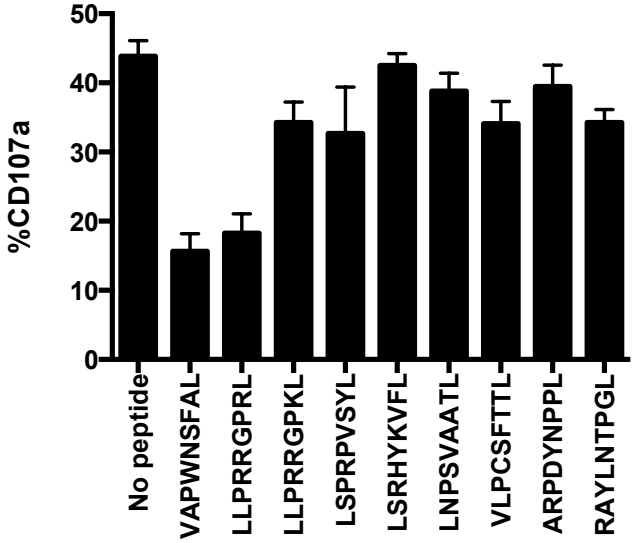

Figure S3: Cytotoxicity of KIR2DS2+ NK cell clones to peptide loaded 721.174 cells

Figure S3A Cell tracker orange (CTO) cytotoxicity assay of 721.174 cells incubated with either no peptide, LNPSVAATL (LNP) or VAPWNSFAL (VAP-FA) and four NK cell clones (three KIR2DS2+ and one KIR2DS2-) at an effector:target ratio of 6:1. Target cells were labeled with CTO and following incubation with NK cell clones for four hours, stained with Live/Dead fixable Aqua dead cell stain. Peptides were used at 100µM**.**

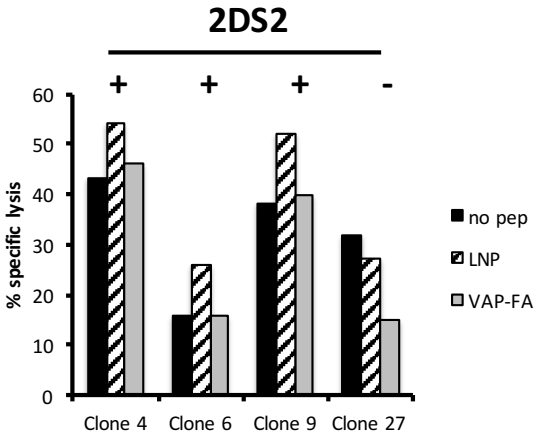

Figure S3B Dot plots for one KIR2DS2+ NK cell clone. Plots are gated on CTO-positive target cells.

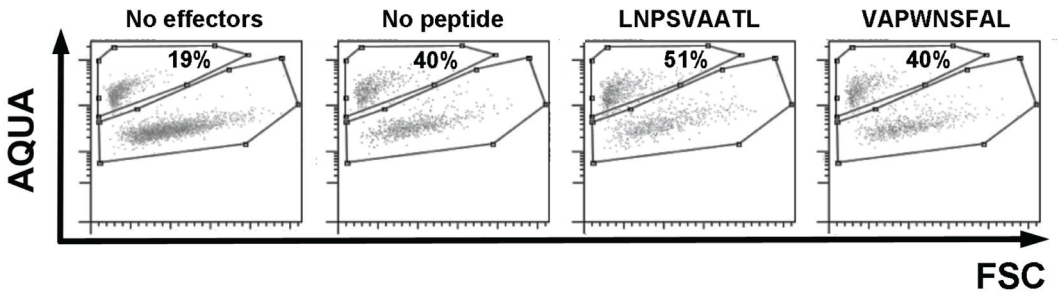

Figure S4: KIR2DS2-tetramer binding to HLA-C*0102 and HCV peptides or VAPWNSLSL peptide derivatives

721.174 cells were cultured overnight with 100μM of the indicated peptides overnight then stained with the KIR2DS2-tetramer and analyzed by flow cytometry.

Figure S4A: Histogram plots for the peptides (red) in comparison to the no peptide control (blue) and the median fluorescence of staining is indicated.

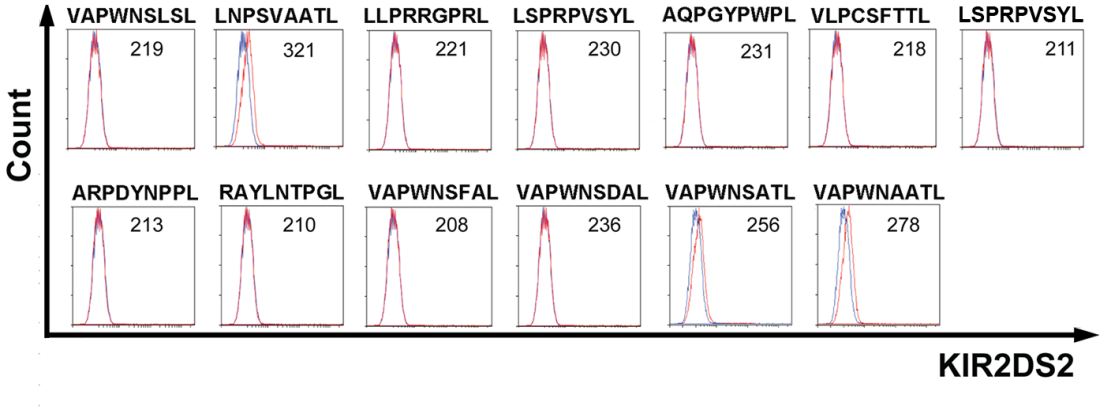

Figure S4B: Summary of three independent KIR2DS2-tetramer binding experiments. The fold increase in binding compared to the no peptide control is indicated: Significant increases in binding compared to the naturally eluted peptides VAPWNSLSL, were noted for the LNPSVAATL peptide and also VAPWNSLSL derivatives with AT at P7 and P8 respectively. *p<0.05, **p<0.001, ***p<0.001 as determined by one-way ANOVA and Dunnett's test for multiple comparisons.

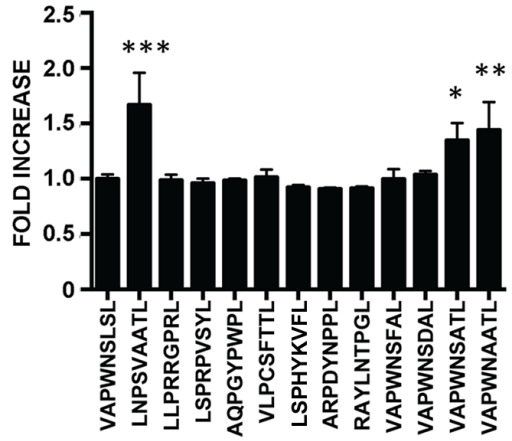

Figure S5: Flow cytometry plots comparing binding of KIR2DS2*001, KIR2DS2*007 and KIR2DS2*008 binding to HLA-C*0102 and peptide

721.174 cells were cultured overnight with 100µM of the indicated peptides, then stained with the indicated KIR2DS2-tetramers and analyzed by flow cytometry. Histograms show binding of tetramers to peptide loaded 721.174 cells (black lines) compared with the no peptide control (gray lines). The median fluorescence intensity of tetramer binding to peptide loaded 721.174 is indicated.

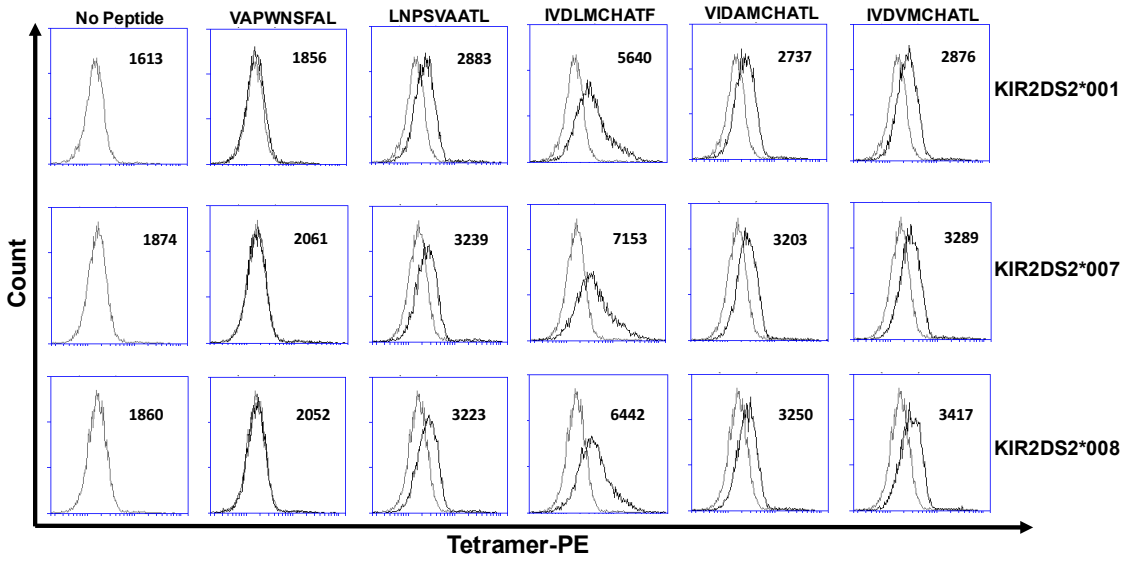

Figure S6: Analysis of viral RNA and protein production in DENV replicon containing cells compared to DENV-2 infected cells.

HEK293T cells either infected with DENV-2 (moi=1), stably expressing a DENV-2 replicon (Rep-DV), or mock infected were harvested at the indicated time points after infection (or the corresponding time points for the replicon and mock infected cells) and used for total RNA and protein extraction.

Fig. S6A: 1 ug of RNA was used for qRT-PCR using the 2X SYBR Green/ROX qPCR Master Mix. The qRT-PCR reaction was performed using the Stratagene MX3005P QPCR System. The Ct (cycle threshold) value for each sample was used for RNA quantification. The ratio of DENV-2 NS5 target gene expression was defined as fold change in target gene expression divided by fold change in reference gene (ACTB) expression.

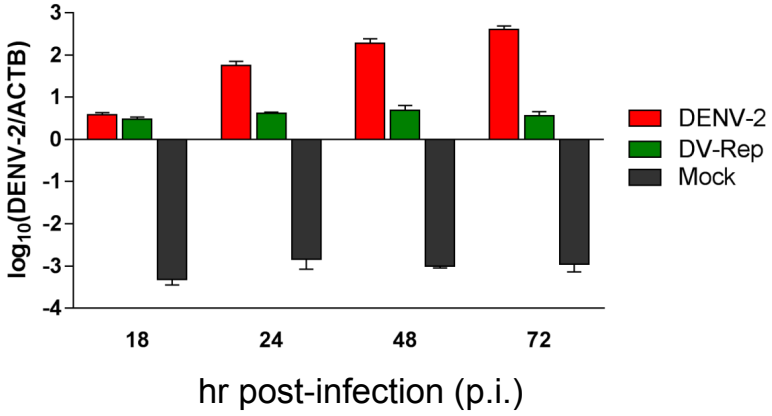

Fig. S6B: Proteins in total cell lysates prepared from the cell samples were separated by 12% SDS-PAGE and analysed by Western blot using anti-NS5 rabbit and anti-GAPDH mouse primary antibodies, a HRP-conjugated anti-rabbit / mouse IgG secondary antibody and a chemiluminescence detection system. The amount of GAPDH was determined as a loading control. The sizes of relevant molecular weight markers (in kDa) are shown.

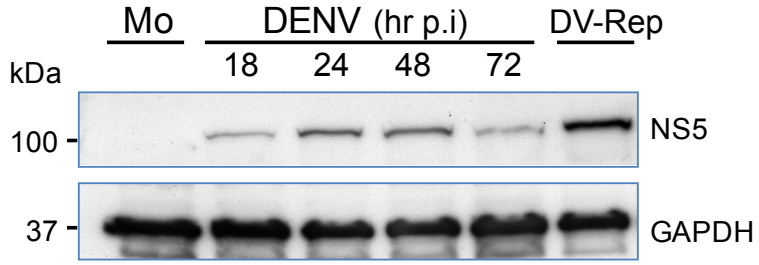

Figure S7: Flow cytometry plots illustrating gating strategy and killing of HEK cells expressing GFP-tagged Dengue virus replicon by NKL-2DS2 cells

HEK cells expressing a dengue virus replicon (HEK:DENV) or HEK-C*0102 cells (HEK:C*0102) expressing a dengue virus replicon (HEK:C*0102:DENV) were co-cultured with NKL cells expressing KIR2DS2 or KIR2DL2 and cytotoxicity assessed at 24 hours using a zombie violet live/dead stain. For the comparison of HEK:C*0102 and HEK:C*0102:DENV, target cells were gated on HLA-C*0102mCherry (**S7A**) and for comparison of HEK:DENV with HEK:C*0102:DENV, target cells were gated on dengue-FITC (**S7B)**

Table S1:

Summary of hepatitis C virus (HCV) peptides identified to bind HLA-C*0102 using the indicated algorithms and compared to the naturally eluted peptide VAPWNSLSL. The genotype 1b virus was used as the template for the screen. Net MHC Pan score is shown as binding affinity, a KISS score of 1 corresponds to binding and of 0 to no binding and for the ADT binding energies a lower score indicates better binding[52-54].

Peptides	Protein	Net MHC Pan peptide binding affinity (nM)	KISS Score	ADT (Binding Energies)
VAPWNSLSL	Host TIMP1	22.70	1	5.919544
VLPCSFTTL	HCV E2	199.73	1	10.485140
LNPSVAATL	HCV NS3	1306.03	0	7.113784
LSPRPVSYL	HCV NS3	276.65	0	7.147722
LLPRRGPRL	HCV Core	296.22	1	8.483209
RAYLNTPGL	HCV NS3	250.21	1	5.517011
AQPGYPWPL	HCV Core	1899.79	1	7.790346
ARPDYNPPL	HCV NS5A	4401.92	1	7.753846
LSPHYKVFL	HCV NS2	5333.43	1	7.521453

Table S2:

Protein sequence alignment of hepatitis C viruses derived from consensus sequences from the Los Alamos HCV sequence database (http://hcv.lanl.gov/). The LNPSVAATL epitope is indicated.

Table S3:

Flavivirus NS3 HLA-C*0102 binding peptides with an “AT” motif at the C terminus minus one and two positions as determined by NetMHCpan 2.8. The naturally eluted self-peptide and HCV NS3 peptide are shown for comparison. Numbering is from the start of the NS3 region. A higher prediction score and a lower percent rank are more likely to be associated with HLA class I binding.

Peptide	ID	Prediction score	Affinity (nM)	Percent Rank
VAPWNSLSL	$TIMP1_{125-133}$	0.4686	314.1935	0.01
IVDVMCHATL	Japanese $encephalitis_{343-352}$	0.2883	2210.1042	0.3
IVDVMCHATL	West Nile $virus_{343-352}$	0.2883	2210.1042	0.3
VIDAMCHATL	Yellow $fever_{338-347}$	0.277	2495.4788	0.4
IVDLMCHATF	$Dengue_{255-264}$	0.2301	4146.1392	1
IVDLMCHATF	$Zika_{310-319}$	0.2301	4146.1392	1
LNPSVAATL	$HCV_{228-236}$	0.1952	6051.6265	2

Table S4: Accession numbers used to compile the *Flavivirus* sequence alignment in Figure 4

Virus	***Gene/protein bank accession number***
Absettarov tick-borne encephalitis	AHM02467.1
Alfuy	AAX82481.1
Apoi	NP_775684.1
Aroa	AIU94739.1
Bagaza	AEI27245.1
Banzi	ABI54472.1
Bouboui	ABI54473.1
Bussuquara	AAV34152.1
Cacipacore	YP_009126874.1
Cowbone Ridge	AAQ14430.1
Dakar bat	AAQ14431.1
Dengue	ACK57817.1
Edge-Hill	ABI54476.1
Entebbe bat	YP_950477.1
Gadgets Gully	ABB90669.1
Hypr Tick-borne encephalitis	AKP16370.1
Ilheus	AGJ84083.1
Israel turkey meningoencephalomyelitis	AGV15509.1
Japanese encephalitis	ABU94628.1
Jugra	ABI54482.1
Jutiapa	AJA91182.1
Kadam	ABB90670.1
Karshi	YP_224133.1
Kedougou	YP_002790882.1
Kokobera	AAV34157.1
Koutango	ABW76844.2
Kumlinge tick-borne encephalitis	ALP82437.1
Kunjin	Pdb:2QEQ
Kyasanur	ADH95737.1
Langat	NP_740299.1
Louping ill	NP_740726.1
Meaban	ABB90668.1
Modoc	AAQ14433.1
Motana myotis leukoencephalitis	NP_775649.1
Murray Valley encephalitis	PDB: 2WV9_A
Naranjal	AIU94742.1
Negishi	ALP82435.1
Ntaya	YP_006846328.2
Omsk hemorrhagic fever	NP_878909.1
Phnom Penh bat	AJA91183.1
Powassan	NP_775520.1
Rio Bravo	NP_776076.1
Rocio	AAV34158.1
Royal farm	ABB90673.1

Saboya	AAQ14435.1
Sal Vieja	AAQ14429.1
Saumarez Reef	ABB90674.1
Sepik	YP_950478.1
Sokoluk]	AHL27154.1
Spondweni	ABI54480.1
St. Louis encephalitis	AGE00046.1
Stratford	AIU94744.1
Tembusu	AGU68254.1
Tick borne encephalitis	AEQ77280.1
Tyuleniy	AHH82586.1
Uganda S	ABI54481.1
Usutu	YP_164814.1
Wesselsbron	AFK88571.1
West Nile	AFI56984.1
Yaounde	ABW76843.2
Yellow-fever	AIZ07887.1
Yokose	BAC79364.1
Zika	BAP47441.1